

# Pressure–temperature phase diagrams of pure and Ag-doped nanocrystalline TiO<sub>2</sub> photocatalysts

M. Stir, R. Nicula\*, E. Burkel

*Institute of Physics, Rostock University, August-Bebel-Str. 55, D-18055 Rostock, Germany*

Received 27 November 2004; received in revised form 1 March 2005; accepted 12 March 2005

Available online 13 June 2005

## Abstract

In situ synchrotron radiation X-ray diffraction methods were used to determine the low pressure–high temperature phase diagrams of nanocrystalline TiO<sub>2</sub> powder specimens obtained using a room temperature sol–gel procedure. Nanostructured Ag-doped bulk titania specimens were pressure sintered and their surface microstructural features (mesoporosity, uniform formation of surface metal clusters) optimized for their envisaged application as photocatalytic materials for air and water decontamination.

© 2005 Elsevier Ltd. All rights reserved.

*Keywords:* Hot-pressing; Sol–gel; Nanocomposites; X-ray methods; TiO<sub>2</sub>

## 1. Introduction

An essential issue in the development and use of nanomaterials in modern applications is the ability to maintain ultrafine particle sizes within extended temperature–pressure ranges. The surface free energy and stress control the thermodynamic phase stability for ultrafine-grained materials. Both these parameters may be fine-tuned by modifying the surface chemistry of the nanoparticles or applied pressure, respectively.<sup>1–5</sup>

Nanocrystalline titanium dioxide (nc-TiO<sub>2</sub>) is known as an excellent semiconductor photocatalyst for environmental protection applications such as the decontamination of polluted waste water and air purification.<sup>6</sup> The photocatalytic efficiency of nc-TiO<sub>2</sub> depends on its crystal structure and surface morphology<sup>7,8</sup> and may further be enhanced by adequate metal-doping and by achieving mesoporous surfaces.<sup>9,10</sup> Nowadays, nanocrystalline TiO<sub>2</sub> also finds important applications in the photo-electrochemical conversion of solar energy,<sup>11</sup> sterilization (anti-bacterial effect),<sup>12</sup> cancer

treatment<sup>6,13</sup> and in the production of self-cleaning and of anti-fogging surfaces (photo-induced hydrophilicity).<sup>14</sup>

The use of semiconductor photocatalysts in supported form (pellets or thin-films) eliminates the need for air-bubbling of the contaminated liquid media (to counteract powder sedimentation) and for subsequent complex photocatalyst powder recycling procedures.

The consolidation of nanosized powders into bulk nanostructured solids is known to be difficult due to their low apparent density, low flow rate, high surface areas and severe interparticle friction of the ultrafine powders.<sup>15,16</sup> The densification and coarsening of nanocrystalline powders was reviewed in several papers.<sup>15–18</sup> Porosity, the formation of metastable phases, the presence of solute elements, the occurrence of structural phase transitions and external pressure influence the sintering behaviour of nanomaterials. Peculiar attention was paid to the modification of thermodynamic phase stability at ultrafine grain-sizes.<sup>19,20</sup> Recently, the new concept of particle-size dependent phase diagrams was developed.<sup>21</sup>

In this paper, we report the pressure-assisted synthesis of Ag-doped bulk nanocrystalline titania, foreseen as high performance self-supported nanomaterial for biomedical applications or semiconductor photocatalysis.<sup>22,23</sup>

\* Corresponding author. Tel.: +49 381 498 6861; fax: +49 381 498 6862.  
E-mail address: [nicula@physik1.uni-rostock.de](mailto:nicula@physik1.uni-rostock.de) (R. Nicula).

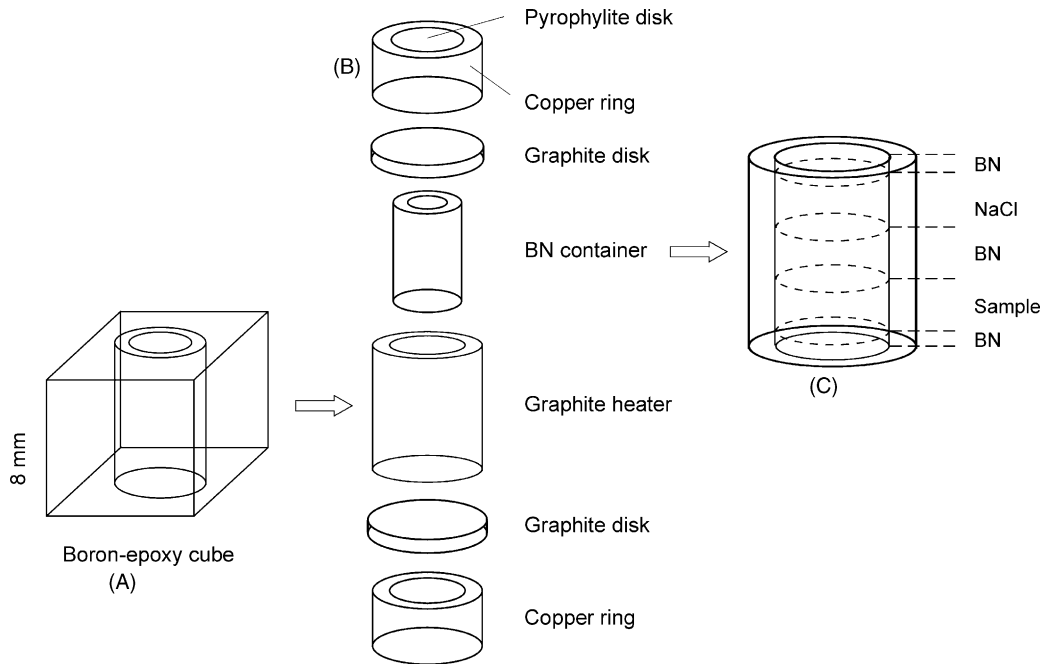


Fig. 1. Schematic diagram<sup>27</sup> of the sample loading procedure: (A) amorphous boron/epoxy resin container; (B) expanded view of the graphite heater, boron nitride sample container and electrical contacts; (C) detail view of the inner BN cylinder containing the specimen and the NaCl pressure marker, separated by BN powder layers.

**2. Experimental**

Pure and Ag-doped titania sols were obtained by the hydrolysis of metal alkoxides route at room temperature. Titanium tetraisopropoxide (TTIP;  $Ti(OC_3H_7)_4$ ) was used

as precursor material. In a typical synthesis of  $TiO_2$ , TTIP (30 mL) is first dissolved in ethanol (EtOH, 100 mL) under vigorous stirring for about 15 min. Distilled water and  $HNO_3$  hydrolysis catalyst (5 mL, 0.1N) are then added to complete the hydrolysis reaction in an ultrasonic bath. The

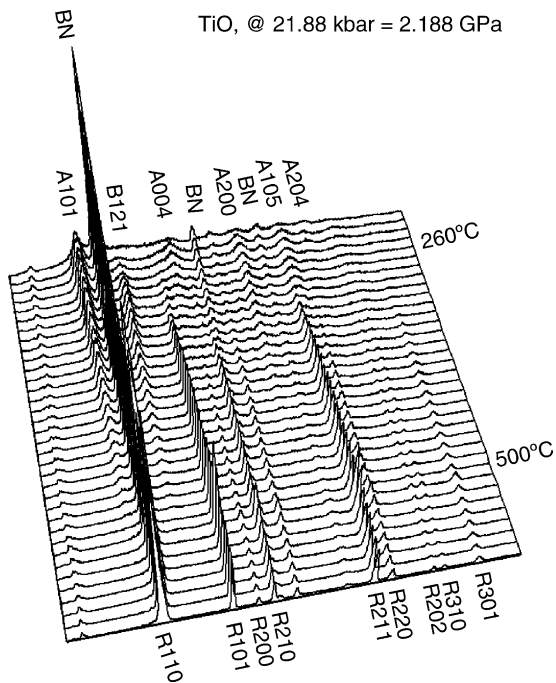


Fig. 2. Energy dispersive X-ray diffraction patterns of nc- $TiO_2$  upon heating at 2.188 GPa.

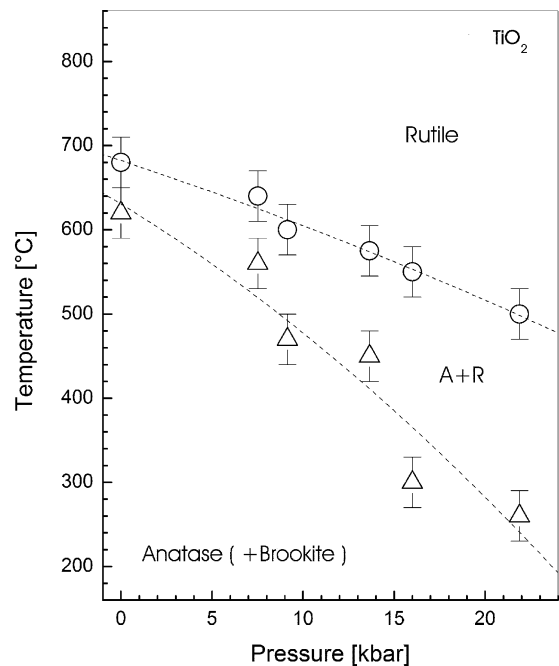


Fig. 3. The pressure–temperature phase diagram of nanocrystalline  $TiO_2$  sol–gel powders. Dotted lines are guides to the eye.

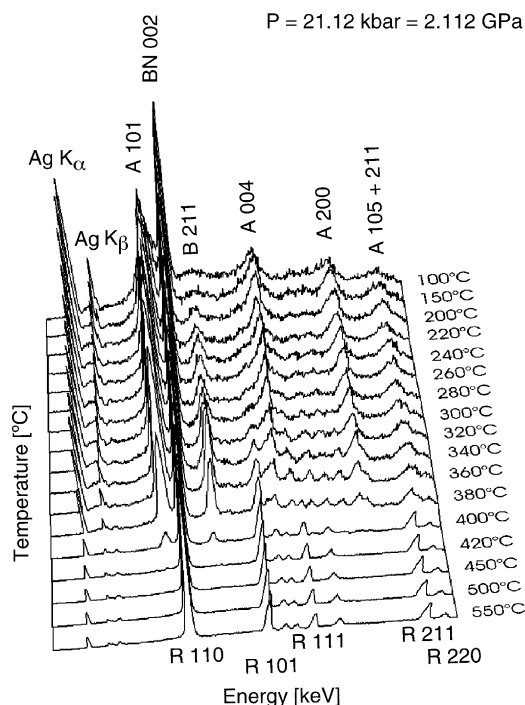


Fig. 4. Energy dispersive X-ray diffraction patterns collected upon constant rate heating of Ag-doped nanocrystalline  $\text{TiO}_2$  at 2.112 GPa.

amount of  $\text{H}_2\text{O}$  was also varied (15–36 mL), corresponding to hydrolysis ratios  $[\text{H}_2\text{O}]/[\text{TTIP}]$  between 8 and 20. The addition of HCl catalyst (35%, 1 mL) during hydrolysis was previously found to suppress the formation of the orthorhombic brookite phase in as-prepared specimens.<sup>25</sup>

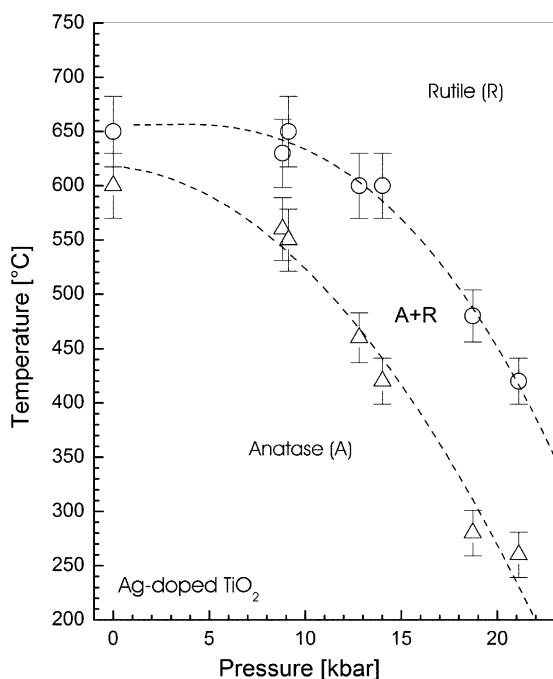


Fig. 5. The pressure–temperature phase diagram of Ag-modified nc- $\text{TiO}_2$  powders. Dotted lines are guides to the eye.

For the synthesis of Ag-doped  $\text{TiO}_2$  specimens, silver nitrate ( $\text{AgNO}_3$ , 4 mL) is also added, as the silver ions source. The solutions were further homogenized for a few hours with a magnetic stirrer, then aged at room temperature. The X-ray diffraction patterns of the as-dried titania powders mainly evidence the formation of the nanocrystalline tetragonal anatase phase: neither traces of noble-metal species or their oxides could be detected in as-prepared specimens, pointing to a highly uniform dispersion of Ag ions within the anatase matrix.<sup>24,25</sup>

The pressure–temperature phase diagrams of nanocrystalline titania powders were determined by in situ synchrotron radiation X-ray diffraction experiments, performed in energy dispersive mode at the MAX80 beamline at HASY-LAB/DESY (Hamburg, Germany).<sup>26,27</sup> The nc- $\text{TiO}_2$  powders are mounted into an amorphous boron/epoxy resin cube container (Fig. 1A). Heating is provided by DC current passing through a graphite cylinder (Fig. 1B). The powders are loaded inside a boron nitride (BN) inner cylinder which also contains the pressure calibration material (NaCl). Boron nitride powder layers further separate the sample from the NaCl pressure marker (Fig. 1C). The powder specimens are thus embodied in a chemically inert environment throughout the X-ray experiment. The in situ diffraction experiments typically consist of isothermal compression at room temperature followed by isobaric heating up to 1300 °C.

Scanning electron microscopy (SEM) and chemical composition analysis using energy dispersive X-ray spectroscopy (EDX) were performed using a Zeiss DSM 960A electron microscope.



Fig. 6. Ag-doped bulk nanocrystalline titania specimens (2 cm diameter, 3 mm thickness).

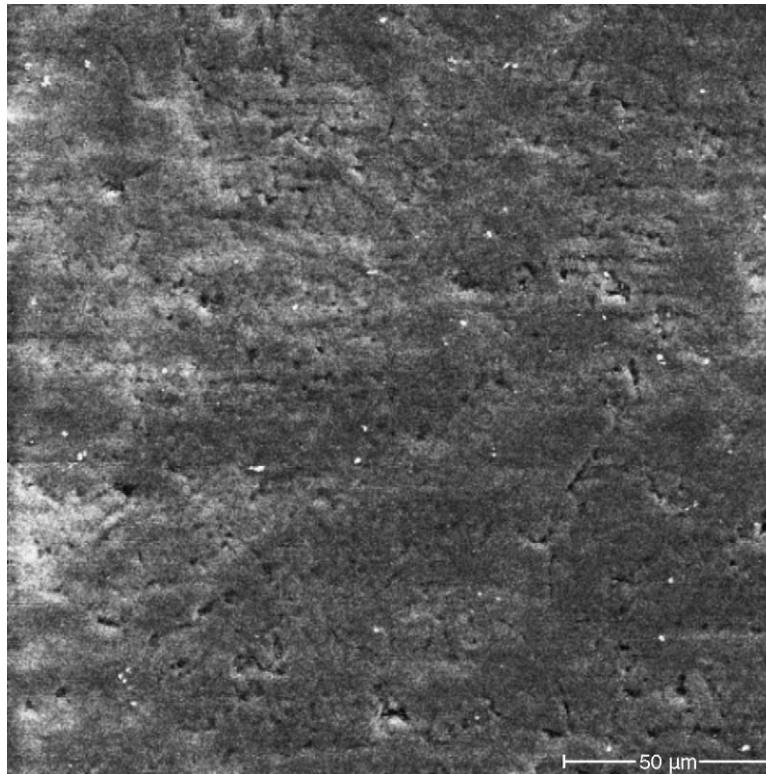


Fig. 7. Typical SEM micrograph of the surface of Ag-modified nanocrystalline TiO<sub>2</sub> pellets.

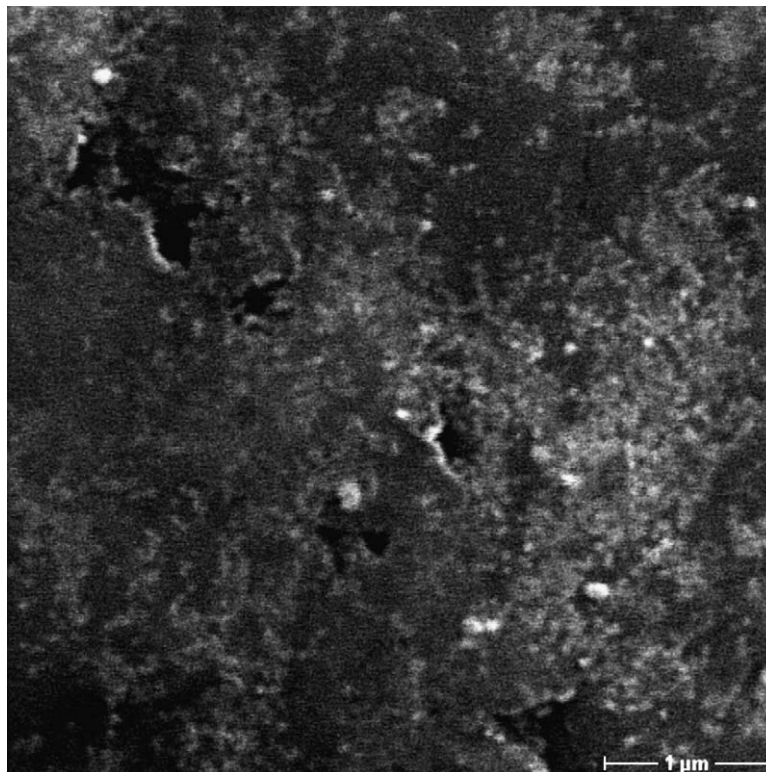


Fig. 8. Higher magnification SEM micrograph of the nanocrystalline Ag-doped TiO<sub>2</sub> surface.



### 3. Results

The sintering behaviour of pure and Ag-doped TiO<sub>2</sub> nanocrystalline powders under constant rate heating and isothermal annealing at ambient pressure was reported in a recent paper.<sup>28</sup> It was found that as-prepared nanocrystalline anatase particles (5–10 nm) do not coarsen significantly under constant rate (2 K/min) heating up to the onset of the anatase-to-rutile transition at about 620 °C. The anatase transformation to rutile is completed above 860 °C for nc-TiO<sub>2</sub> and at only 740 °C for the Ag-modified specimens.

The in situ X-ray diffraction patterns recorded during heating of nc-TiO<sub>2</sub> powders under an applied pressure of 2.188 GPa are shown in Fig. 2. A strong reduction (down to only 260 °C) of the onset temperature of the anatase–rutile transformation is observed. The transition is completed at 500 °C. Fig. 3 illustrates the experimental pressure–temperature phase diagram for the nc-TiO<sub>2</sub> powders.

For the Ag-modified TiO<sub>2</sub> nanopowders, the onset temperature of the anatase-to-rutile transformation also decreases down to 250 °C at pressure values close to 2 GPa (Fig. 4). The Ag fluorescence lines are also observed. The transformation is completed already at 420 °C. The experimental pressure–temperature phase diagram of Ag-doped TiO<sub>2</sub> samples for the low pressure range up to 2.3 GPa is shown in

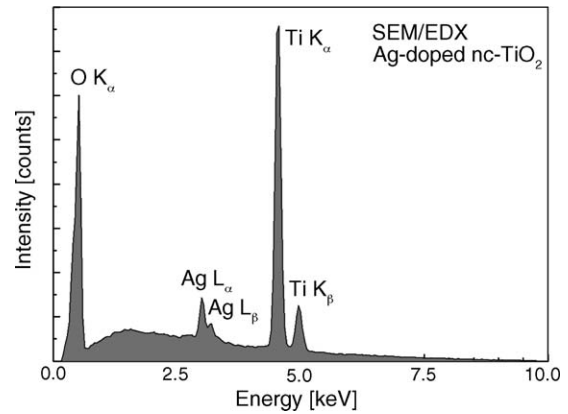


Fig. 9. Energy dispersive (SEM/EDX) chemical composition analysis of Ag-modified nc-TiO<sub>2</sub> (pellet surface, 5 μm × 5 μm area).

Fig. 5. The pressure-induced decrease of the transformation temperatures in nanocrystalline titania can be attributed to the lowering of the thermodynamic barrier for nucleation for pressures above a certain (temperature dependent) critical pressure value.<sup>16,24</sup>

In view of the strong particle-size dependence of the transformation temperatures in nanomaterials, the experimental determination of their phase diagrams appears to condition

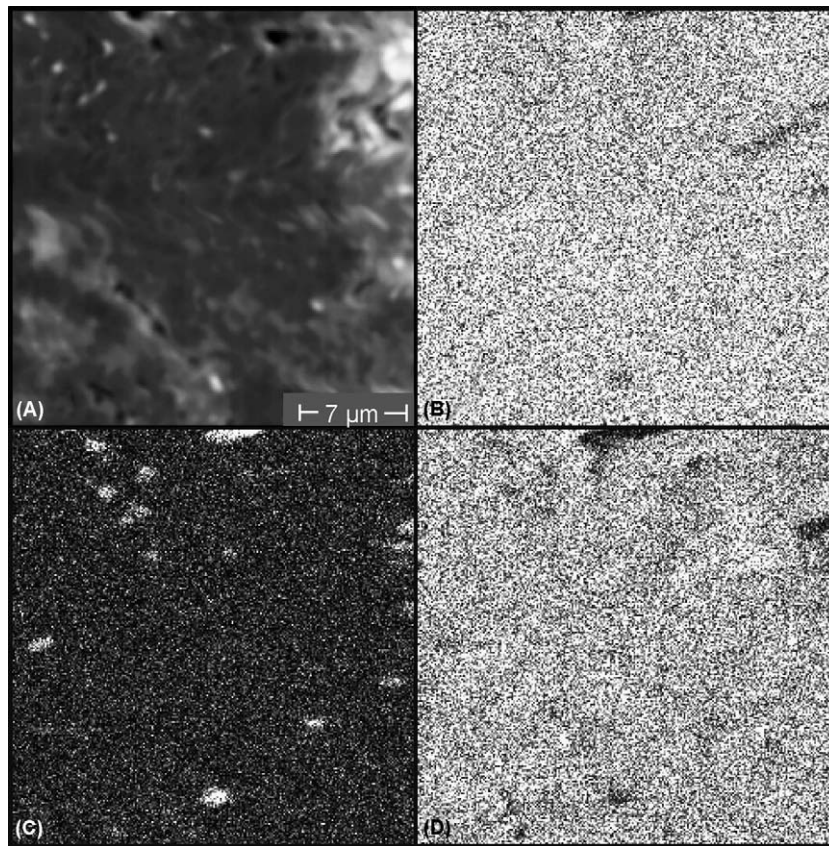


Fig. 10. Chemical composition maps for the surface area shown in the bright-field image (A). The distribution of Ti (B), Ag (C) and oxygen (D) demonstrates the formation of Ag-rich surface nanoclusters.

the synthesis of bulk nanocrystalline solids from ultrafine powders by means of temperature- and pressure-assisted sintering procedures. Following the pressure–temperature phase diagrams of nanocrystalline TiO<sub>2</sub> (Figs. 3 and 5), bulk pellets (2 cm diameter, 3 mm thickness) were prepared by hot-pressing (Fig. 6).

Typical scanning electron microscopy micrographs (Fig. 7) of Ag-modified nc-TiO<sub>2</sub> pellets prepared using external uniaxial pressures close to 1 GPa evidence the retention of uniform surface mesoporosity (pore sizes up to several microns), a highly desirable feature for their foreseen application as photocatalyst materials for air and waste water decontamination.

At further magnifications, the SEM micrographs prove the formation of nanocrystalline grains with an average size of about 80 nm (Fig. 8). Composition analysis (SEM/EDX) performed over an area of 5 μm × 5 μm (Fig. 9) reveals the expected noble-metal content (of about 3% Ag).

In addition, chemical composition maps (Fig. 10) were obtained in order to identify the nature of the surface nanoparticles (Figs. 8 and 10A). The spatial distribution of titanium (Fig. 10B), silver (Fig. 10C) and oxygen (Fig. 10D) elements corresponding to the surface area (20 μm × 20 μm) in Fig. 10A evidences the formation of Ag-rich clusters on the surface of the nanostructured titania pellets. A certain amount of Ag ions remains, however, uniformly distributed within the TiO<sub>2</sub> matrix (Fig. 10C). The silver-rich surface clusters have submicron sizes and are uniformly distributed over the pellet surface of the TiO<sub>2</sub> photocatalyst. This particular microstructural feature of our Ag-doped bulk nanocrystalline TiO<sub>2</sub> specimens is expected to contribute to the overall improvement of their photocatalytic efficiency. Further experiments are underway to certify the above assumption for several photocatalytic reactions of interest.

#### 4. Conclusions

Amorphous and nanostructured titania xerogels with grain-sizes below 10 nm were prepared using room temperature sol–gel procedures. Sol–gel processing offers the unique advantage of achieving uniform distributions of doping elements within a given matrix at molecular level. The pressure dependence of the crystallization and/or solid-state transformation temperatures of as-prepared ultrafine nanopowders was investigated using in situ synchrotron radiation diffraction to obtain pressure–temperature phase diagrams in the low pressure–high temperature region up to 2.3 GPa and 1300 °C, respectively. Pressure was found to lower the onset temperature of the anatase-to-rutile transition down to approximately 250 °C at pressures close to 2 GPa, due to its effect on the energy barrier for nucleation. As a direct consequence, pressure-assisted processing methods may further be employed to obtain nanostructured bulk TiO<sub>2</sub>-based specimens using pressure equipment largely available in research laboratories or industry.

Energy bandgap modification by metal-doping is nowadays foreseen as one of the main ways to enhance the activity of semiconductor photocatalysts and to extend their efficiency to the visible light range. Special attention was therefore here given to the synthesis and surface properties of Ag-doped TiO<sub>2</sub> photocatalyst materials. The main aim was to promote the uniformly distributed formation of surface noble-metal clusters that may act as local trapping centers for the charge carriers. Noble-metal clusters may further assist spatial charge separation, thus suppressing or delaying recombination processes and promoting an enhanced photocatalytic activity of the nanomaterial. Under ambient pressure, Ag clusters were previously found to form only at elevated temperatures above 750 °C, at which the initial anatase titania matrix already completely transformed to the less photoactive rutile phase.<sup>24</sup> In contrast, we could here show that – based on the experimental pressure–temperature phase diagrams – pressure-assisted powder processing routes may be used to obtain nanostructured Ag-doped titania bulk specimens with predefined ratios of anatase–rutile phase constituents. While an amount of Ag ions remain uniformly distributed within the nanocrystalline TiO<sub>2</sub> matrix, submicron sized Ag-rich clusters were shown to form on the surface of consolidated titania pellets. Mesoporous surfaces were retained for appropriate choices of the external pressure used for densifying the ultrafine titania powders.

#### Acknowledgements

The authors gratefully acknowledge the help of Dr. T. Traykova with sample preparation. Thanks are due to Dr. C. Lathe for support at the F2.1 beamline in HASYLAB. We would also like to thank Prof. Dr. L. Jonas and Ing. G. Fulda (Electron Microscopy Center, Rostock University) for assistance with the SEM/EDX experiments.

#### References

1. Gleiter, H., Nanostructured materials: state of the art and perspectives. *Nanostruct. Mater.*, 1995, **6**, 3–14.
2. Gleiter, H., Nanostructured materials: basic concepts and microstructure. *Acta Mater.*, 2000, **48**, 1–29.
3. Bourell, D. L., ed., *Synthesis and Processing of Nanocrystalline Powder*. TMS, Warrendale, PA, 1996.
4. Nastasi, M., Parkin, D. M. and Gleiter, H., ed., *Mechanical Properties and Deformation Behavior of Materials having Ultra-Fine Microstructures*. Kluwer Acad. Publ, Dordrecht, The Netherlands, 1993.
5. Edelstein, A. S. and Cammarata, R. C., ed., *Nanomaterials: Synthesis, Properties and Applications*. IoP Publ, Bristol, 1996.
6. Fujishima, A., Rao, T. N. and Tryk, D. A., Titanium dioxide photocatalysis. *J. Photochem. Photobiol. C: Photochem. Rev.*, 2000, **1**, 1–21.
7. Diebold, U., The surface science of titanium dioxide. *Surf. Sci. Rep.*, 2003, **48**, 53–229.

8. Hoffman, M. R., Martin, S. T., Choi, W. and Bahnemann, D. W., Environmental applications of semiconductor photocatalysis. *Chem. Rev.*, 1995, **95**, 69–96.
9. Yusuf, M. M., Imai, H. and Hirashima, H., Preparation of mesoporous titania by templating with polymer and surfactant and its characterization. *J. Sol–Gel Sci. Technol.*, 2003, **28**, 97–104.
10. Zhang, Y., Weidenkaff, A. and Reller, A., Mesoporous structure and phase transition of nanocrystalline TiO<sub>2</sub>. *Mater. Lett.*, 2002, **54**, 375–381.
11. O'Regan, B. and Grätzel, M., A low-cost, high-efficiency solar cell based on dye-sensitized colloidal TiO<sub>2</sub> films. *Nature*, 1991, **353**, 737–739.
12. Sunada, K., Kikuchi, Y., Hashimoto, K. and Fujishima, A., Bactericidal and detoxification effects of TiO<sub>2</sub> thin film photocatalysts. *Environ. Sci. Technol.*, 1998, **32**, 726–728.
13. Fujishima, A., Hashimoto, K. and Watanabe, T., *TiO<sub>2</sub> Photocatalysis: Fundamentals and Applications*. BKC, Tokyo, 1999.
14. Mills, A. et al., Thick titanium dioxide films for semiconductor photocatalysis. *J. Photochem. Photobiol. A: Chem.*, 2003, **160**, 185–194.
15. Groza, J. R. and Dowding, R. J., Nanoparticulate materials densification. *Nanostruct. Mater.*, 1996, **7**, 749–768.
16. Liao, S. C., Mayo, W. E. and Pae, K. D., Theory of high pressure/low temperature sintering of bulk nanocrystalline TiO<sub>2</sub>. *Acta Mater.*, 1997, **45**, 4027–4040.
17. Groza, J. R., Nanosintering. *Nanostruct. Mater.*, 1999, **12**, 987–992.
18. Kim, H. G. and Kim, K. T., Densification behavior of nanocrystalline titania powder compact under high temperature. *Acta Mater.*, 1999, **47**, 3561–3570.
19. Zhang, H. and Banfield, J. F., Thermodynamic analysis of phase stability of nanocrystalline titania. *J. Mater. Chem.*, 1998, **8**, 2073–2076.
20. Zhang, H. and Banfield, J. F., Understanding polymorphic phase transformation behaviour during growth of nanocrystalline aggregates: insights from TiO<sub>2</sub>. *J. Phys. Chem. B*, 2000, **104**, 3481–3487.
21. Mayo, M. J., Suresh, A. and Porter, W. D., Thermodynamics for nanosystems: grain and particle-size dependent phase diagrams. *Rev. Adv. Mater. Sci.*, 2003, **5**, 100–109.
22. Chao, H. E., Yun, Y. U., Xingfang, H. U. and Larbot, A., Effect of silver doping on the phase transformation and grain growth of sol-gel titania powder. *J. Eur. Ceram. Soc.*, 2003, **23**, 1457–1464.
23. Falaras, P., Arabatzis, I. M., Stergiopoulos, T. and Bernard, M. C., Enhanced activity of silver modified thin-film TiO<sub>2</sub> photocatalysts. *Int. J. Photoenergy*, 2003, **5**, 123–130.
24. Stir M., Structure and dynamics of amorphous and nanostructured materials. Ph.D. Thesis, University of Rostock, 2004.
25. Nicula, R., Stir, M., Schick, C. and Burkel, E., High-temperature high-pressure crystallization and sintering behaviour of brookite-free nanostructured titanium dioxide: in situ experiments using synchrotron radiation. *Thermochim. Acta*, 2003, **403**, 129–136.
26. Buras, B. and Gerward, L., *Prog. Crystal Growth Charact.*, 1989, **18**, 93–138.
27. Staun-Olsen, J., Gerward, L. and Jiang, J. Z., On the rutile/α-PbO<sub>2</sub>-type phase boundary of TiO<sub>2</sub>. *J. Phys. Chem. Solids*, 1999, **60**, 229–233.
28. Nicula, R., Stir, M. and Burkel, E., Synchrotron radiation investigation of thermal stability and grain-growth in pure and metal-doped nanocrystalline TiO<sub>2</sub>. *Mater. Sci. Forum*, 2004, **467–470**, 1307–1312.